Hindawi
International Journal of Chemical Engineering
Volume 2018, Article ID 6568548, 10 pages
https://doi.org/10.1155/2018/6568548

Research Article

Study of the Equilibrium, Kinetics, and Thermodynamics of Boron Removal from Waters with Commercial Magnesium Oxide

Javier Paul Montalvo Andia,[1] **Lidia Yokoyama**,[2] **and Luiz Alberto Cesar Teixeira**[3]

[1]*Instituto de Energía y Medio Ambiente, Universidad Católica San Pablo, Arequipa, Peru*
[2]*Escola de Química, Departamento de Processos Inorgânicos, Universidade Federal do Rio de Janeiro, Rio de Janeiro, RJ, Brazil*
[3]*Departamento de Engenharia Química e de Materiais, Pontifícia Universidade Católica do Rio de Janeiro, Rio de Janeiro, RJ, Brazil*

Correspondence should be addressed to Lidia Yokoyama; lidia@eq.ufrj.br

Received 20 March 2018; Accepted 8 May 2018; Published 11 June 2018

Academic Editor: Gianluca Di Profio

In the present work, the equilibrium, thermodynamics, and kinetics of boron removal from aqueous solutions by the adsorption on commercial magnesium oxide powder were studied in a batch reactor. The adsorption efficiency of boron removal increases with temperature from 25°C to 50°C. The experimental results were fitted to the Langmuir, Freundlich, and Dubinin–Radushkevich (DR) adsorption isotherm models. The Freundlich model provided the best fitting, and the maximum monolayer adsorption capacity of MgO was 36.11 $mg \cdot g^{-1}$. In addition, experimental kinetic data interpretations were attempted for the pseudo-first-order kinetic model and pseudo-second-order kinetic model. The results show that the pseudo-second-order kinetic model provides the best fit. Such result suggests that the adsorption process seems to occur in two stages due to the two straight slopes obtained through the application of the pseudo-first-order kinetic model, which is confirmed by the adjustment of the results to the pseudo-second-order model. The calculated activation energy (E_a) was 45.5 $kJ \cdot mol^{-1}$, and the values calculated for $\Delta G°$, $\Delta H°$, and $\Delta S°$ were −4.16 $kJ \cdot mol^{1}$, 21.7 $kJ \cdot mol^{-1}$, and 87.3 $kJ \cdot mol^{-1}$, respectively. These values confirm the spontaneous and endothermic nature of the adsorption process and indicated that the disorder increased at the solid-liquid interface. The results indicate that the controlling step of boron adsorption process on MgO is of a physical nature.

1. Introduction

The exploration and production of petroleum from marine subsoil generate large amounts of liquid effluents, also known as produced water, extracted along with crude oil [1]. Produced water is the water found along with oil in the marine reservoir or the water injected into the reservoir in order to recover petroleum. The produced water flow is low at the early stages of production of the reservoir. Nevertheless, it can reach up to 80% of the crude oil extraction in the final years of exploitation of the well [2].

The produced water composition can vary according to the well and usually contains high salinity, organic and inorganic substances, and levels of dissolved solids over 40%, which makes it toxic to the environment [2, 3].

Boron is an element present in the produced water, and its concentration may vary from 4 $mg \cdot L^{-1}$ to 350 $mg \cdot L^{-1}$ [3, 4]. Although boron is considered a micronutrient essential to the development of microorganisms, plants, microalgae, and animals, this element can be toxic at concentration of 0.3 $mg \cdot L^{-1}$ to sensitive plants, at 2 $mg \cdot L^{-1}$ to semitolerant ones, and at 4 $mg \cdot L^{-1}$ to tolerant ones. Therefore, this is one of the reasons why boron is required to be removed from water and other effluents by environmental protection agencies [5, 6].

The maximum boron concentration recommended by the World Health Organization (WHO) for potable water was 0.5 $mg \cdot L^{-1}$ in 1998. However, this value was modified to 2.4 $mg \cdot L^{-1}$ in 2011. According to standards set by legislation, the limit allowed by the European Union, the UK, and Japan

is 1.0 mg·L^{-1}. In South American countries such as Brazil and Peru, the limits for fresh water and wastewater are 0.5 mg·L^{-1} and 5 mg·L^{-1}, respectively. On the contrary, in the USA, the limit is not subject to federal regulations on this issue. The states of Minnesota, Florida, and California have allowed limits of 0.6, 0.63, and 1 mg·L^{-1}, respectively [7–11].

Consequently, the produced water containing boron requires treatment before being released back into the sea or being employed as a hydrosource of potable water.

There are many possible treatments for the boron removal such as the electrocoagulation, process which achieved efficiencies over 98% from synthetic solutions and real produced waters with initial boron concentration between 10 and 30 mg·L^{-1} [12]. Other treatments are the adsorption by different types of adsorbents, including activated carbon, fly ash, clay, mesoporous silica, oxides, nanoparticles, biological material, layered double hydroxides, and natural minerals [13–15]. Some additional methods studied at laboratory, for example, electrodialysis [16], phytoremediation [17, 18], and bioelectrochemical systems, presented removal efficiencies up to 90% [19, 20].

However, the most extensive processes employed for boron removal from produced water and seawater, on a larger scale, are reverse osmosis and ion exchange [21, 22].

As far as reverse osmosis is concerned, boron removal can reach values of 98% at pH = 10.5 since, at this pH, the predominant boron specie is a borate ion $B(OH)^{4-}$ that has a negative charge and larger size when compared to the boric acid (H_3BO_3) [2, 22]. In the case of ion exchange, the removal of boron occurs via its adsorption in specific resins, which are usually synthesized by means of macroporous cross-linked polystyrene resins, and functionalized by the N-methyl-D-glucamine (1-amino-1-deoxy-D-glucitol; NMDG) group achieving removal efficiencies up to 99% [23–26].

The most common commercial resins used in ion exchange process are Diaion CRB 02, Purolite S 108, and Amberlite IRA-743 [6, 27–30].

In general, the initial concentration of boron in produced waters treated with resins can vary between 15 and 60 mg·L^{-1}. However, after a certain period of time, this resin saturates, reaching the breakthrough, and needs to be regenerated to be reused [12, 31].

Regeneration step consists of passing an acid solution (usually H_2SO_4) through a saturated resin, resulting in an acid solution with high concentration of boron, usually between 350 and 700 mg·L^{-1}, which must also be treated.

The volume of this effluent containing boron is relevant when it refers by example to oil waterway terminals, such as São Sebastião Waterway Terminal from Petrobras/Brazil, with a capacity of 1,585,345 m^3 [32]. Due to their magnitude, they generate a large quantity of effluent, which is product of the elution of the resins used at wastewater treatment plants of these terminals.

The treatment of this effluent by conventional technologies is not adequate due to the high concentration of boron. Therefore, under this circumstance, technologies such as precipitation or adsorption seem to be viable alternatives.

Through these treatments, boron concentration could be reduced up to 15–30 mg·L^{-1} that may allow the mixing of treated effluent with production water and these could be subsequently treated by ion exchange resins or reverse osmosis. The resulting solid residue of precipitation/adsorption process can be disposed in landfills or be used as raw material in the manufacture of glass due to its high content of boron. In this context, magnesium oxide is provided as a good alternative as it is environmentally friendly, cost-effective, and nontoxic. Furthermore, it shows low solubility in water, and it is an effective sorbent for the removal of contaminants such as fluoride and toxic dyes [33, 34].

The aim of the present work was to evaluate the kinetics, thermodynamics, and equilibrium of boron removal from aqueous solutions with high content (350 mg·L^{-1}) through adsorption in magnesium oxide.

2. Experimental

2.1. Materials and Methods. For each experiment, a synthetic solution of 350 mg·L^{-1} was prepared by dissolution of boric acid (H_3BO_3) PA in distilled water. The pH of the solution was adjusted with 1 M NaOH and/or 1 M HCl solutions provided by Sigma-Aldrich.

The magnesium oxide used in the adsorption process was supplied by Magnesita SA (MgO-500).

2.2. Characterization of MgO and Boron Concentration Analysis. The sizes of the MgO particles were analyzed by a dual laser liquid dry dispersion particle size analyzer, CILAS 1064L. Boron concentrations in aqueous solutions were determined by optical emission spectrometry analysis with inductively coupled plasma from PerkinElmer, Optima 4300DV. The morphology of the MgO was determined by scanning electron microscopy (MRV).

2.3. Experimental Procedure. The experiments were carried out in a batch reactor with 500 mL of solution. The use of borosilicate glass beaker was to prevent further contamination by dissolution of boron substances from the silicate material (beaker), mainly because the experiments were performed at alkaline pH. The solution was stirred at a speed of 150 rpm, 40 g·L^{-1} of MgO was added, and the pH was readily adjusted after starting the experiment. The pH of the solution was measured using a pH meter (Bel Engineering W3B) and adjusted with 1 M NaOH and/or 1 M HCl solutions (Sigma-Aldrich).

The study of reaction kinetic was performed by collecting the sample every 5 minutes. The samples were vacuum-filtered through a cellulose nitrate membrane of 0.4 μm pore diameter (Nalgene). After 240 minutes of reaction, the stirring was turned off.

The filtered samples were kept for boron concentration analysis by inductively coupled plasma spectrometer (Optima 4300DV, from PerkinElmer).

Simultaneously, a sludge sample was dried at 70°C and adequately stored for further analysis of the surface morphology by scanning electron microscopy (MRV).

Table 1: Chemical composition of MgO-500 (Magnesita SA).

Reagent/composition	Surface area (S_{BET}) ($m^2 \cdot g^{-1}$)	MgO (%)	Fe_2O_3 (%)	Al_2O_3 (%)	SiO_2 (%)	MnO (%)	CaO (%)
MgO-500	31.47	98	0.4	0.1	0.15	0.1	0.9

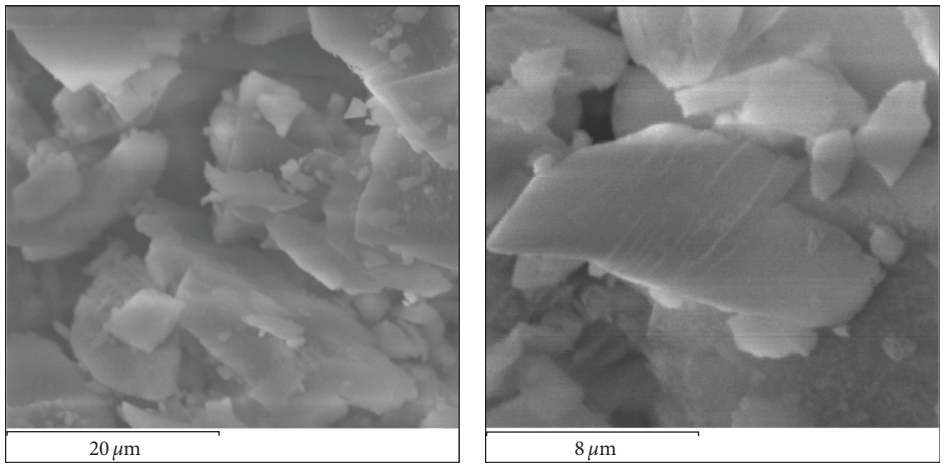

Figure 1: Scanning electron microscope microphotography of MgO-500 before the adsorption process: (a) 20 μm and (b) 8 μm.

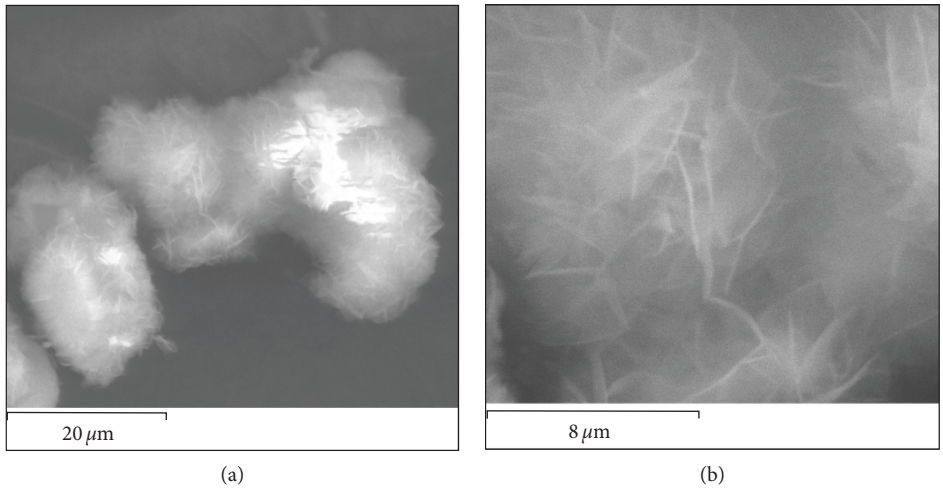

Figure 2: Scanning electron microscope microphotography of MgO-500 after the adsorption process: (a) 20 μm and (b) 8 μm.

The effect of temperature was evaluated in the process of boron removal at range of 5°C to 50°C, with initial concentration of boron of 350 $mg \cdot L^{-1}$. For constant temperature maintenance during the experiments, a cooling or heating system was used.

2.3.1. Adsorption Isotherms. The experiments for adsorption isotherm evaluation were carried out in a batch system with MgO concentration range of 8 $g \cdot L^{-1}$ to 64 $g \cdot L^{-1}$ at three different temperatures of 25°C, 40°C, and 50°C, during 240 min of reaction.

The initial concentration of boron was 350 $mg \cdot L^{-1}$, the stirring speed was 150 rpm, the pH was 10, the temperature was at 25°C, and the volume of the solution was 500 mL. After filtration, the samples were sent to boron concentration analysis.

3. Results and Discussions

3.1. Characterization of MgO. The chemical composition provided by the manufacturer is shown in Table 1.

Figures 1 and 2 show the surface morphology of MgO-500 before and after the adsorption process, respectively. The difference in structure presented in Figure 2 was due to the formation of a layer of H_3BO_3 on the surface of MgO and the hydration of MgO into $Mg(OH)_2$ after the adsorption process.

3.2. Adsorption Isotherms. The adsorption isotherms describe the equilibrium between the concentration of a material in aqueous phase and its concentration on the surfaces

of particle adsorbents. This study employed the Langmuir, Freundlich, and Dubinin–Radushkevich models to describe the equilibrium adsorption.

3.2.1. Dubinin–Radushkevich Isotherm. Dubinin–Radushkevich (DR) isotherm is a model that considers the adsorption in multilayers and in the heterogeneous surfaces.

DR model is expressed mathematically as follows:

$$\ln C_s = \ln X_m - k\,\epsilon^2, \tag{1}$$

where C_s is the amount of boron adsorbed per MgO ($mg{\cdot}g^{-1}$), X_m is the maximum adsorption capacity, k is the constant related to sorption energy ($mol^2{\cdot}kJ^{-2}$), and ϵ is the Polanyi potential. ϵ and E are expressed by (2) and (3), respectively [35]:

$$\epsilon = RT \ln\left(1 + \frac{1}{C_e}\right), \tag{2}$$

$$E = \sqrt{\frac{1}{2k}}, \tag{3}$$

where R is the gas constant ($J{\cdot}mol^{-1}\ K^{-1}$) and T is the temperature (K). E ($kJ{\cdot}mol^{-1}$) is the sorption energy, and the magnitude of its value indicates if the adsorption is of chemical or physical nature.

3.2.2. Langmuir Isotherm. The Langmuir isotherm is a model that considers monolayer adsorption onto a uniform surface with a finite number of adsorption sites and uniform adsorption energy, and this model is given by the following equation [36]:

$$q_e = \frac{K_L q_{max} C_e}{1 + K_L C_e}. \tag{4}$$

Equation (4) can be linearized as follows:

$$\frac{C_e}{q_e} = \frac{C_e}{q_{max}} + \frac{1}{q_{max} K_L}, \tag{5}$$

where C_e is the equilibrium concentration of boron in solution ($mg{\cdot}L^{-1}$), q_e is the quantity of boron adsorbed onto the MgO ($mg{\cdot}g^{-1}$), q_{max} is the maximum monolayer adsorption capacity of MgO ($mg{\cdot}g^{-1}$), and K_L is the Langmuir adsorption constant related to the energy sorption ($L{\cdot}mg^{-1}$).

3.2.3. Freundlich Isotherm. This model is applied to the sorption processes on heterogeneous surfaces and reversible adsorption and admits multilayer adsorption [37].

The Freundlich equation and its linear form can be given as follows:

$$q_e = K_F C_e^{1/n},$$
$$\log q_e = \log K_F + \left(\frac{1}{n}\right)\log C_e, \tag{6}$$

where q_e is the boron concentration adsorbed at equilibrium ($mg{\cdot}g^{-1}$), C_e is the equilibrium concentration of boron in solution ($mg{\cdot}L^{-1}$), and K_F ($L{\cdot}g^{-1}$) and n are the Freundlich sorption isotherm constants, related to the adsorption capacity and the adsorption intensity, respectively.

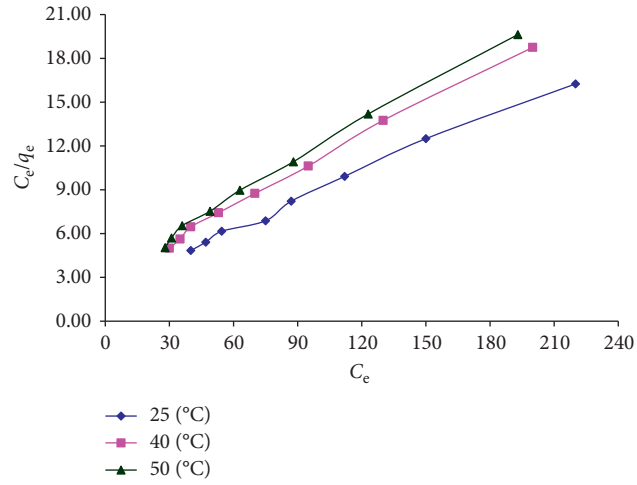

Figure 3: Adsorption isotherms of boron MgO at 25°C, 40°C, and 50°C.

Table 2: Parameters for the isotherms obtained from the Langmuir, Freundlich, and Dubinin–Radushkevich models at 25°C, 40°C, and 50°C, respectively.

Temperature (°C)	Langmuir			Freundlich			DR
	q_{max} ($mg{\cdot}g^{-1}$)	B ($mg{\cdot}L^{-1}$)	R^2	n	K_F	R^2	R^2
25	34.72	0.004	0.91	1.392	0.33	0.99	0.84
40	35.08	0.005	0.93	1.476	0.51	0.99	0.83
50	36.11	0.006	0.93	1.481	0.57	0.99	0.83

DR: Dubinin–Radushkevich isotherm. Initial boron concentration = 350 $mg{\cdot}L^{-1}$, stirring speed = 150 rpm, pH = 10, and t = 240 min.

Figure 3 shows the adsorption isotherms of boron MgO-500 at 25°C, 40°C, and 50°C.

It can be observed that the adsorption isotherm at 25°C could be classified as an H4-type isotherm according to the classification of Giles et al. [38]. This type of isotherm suggests a high affinity between adsorbate-adsorbent, and the subgroup 4 suggests the formation of monolayers of adsorbate on the surface of adsorbent.

On the contrary, for the isotherms at 40°C and 50°C, it is observed that they are similar L-type isotherms according to the classification of Giles et al. [38].

This type of isotherm assumes the existence of an affinity between ion $B(OH)^{4-}$ and MgO, and if more sites of the adsorbent are filled, it will be more difficult to fill the empty sites with other solute molecules. This type of isotherm is commonly represented under the following mechanism: (1) molecules are adsorbed in layers and (2) there is competition for the active sites on the adsorbent surface between adsorbate molecules and solvent molecules [39–41].

In the present work, the Langmuir, Freundlich, and Dubinin–Radushkevich models were evaluated, which are the most widely used models to describe an adsorption process.

According to the results shown in Table 2, the model that provides a better fit to the experimental data is the isotherm

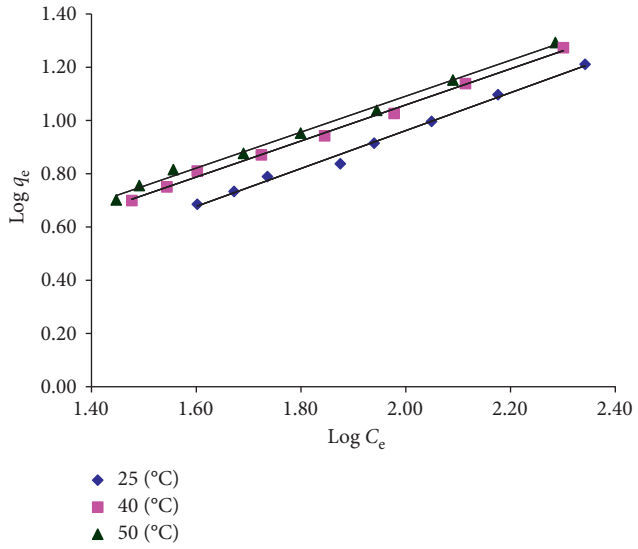

Figure 4: Data adjustment of the adsorption isotherms for the Freundlich model at temperatures of 25°C, 40°C, and 50°C. Initial boron concentration = 350 mg·L^{-1}, stirring speed = 150 rpm, pH = 10, and t = 240 min.

of Freundlich at 25°C, 40°C, and 50°C with 99% correlation. Figure 4 shows the data adjusting to the Freundlich isotherm, and Table 3 compares the Freundlich isotherm parameters between MgO used at present work and other adsorbents.

The Freundlich isotherms suggest a heterogeneous adsorbent surface and a reversible adsorption process, which considers the formation of multilayer. However, the adsorption of ion $B(OH)^{4-}$ may involve different mechanisms, such as ion exchange, microprecipitation, complexation/chelation, and electrostatic attraction [40–42].

The Freundlich isotherms were obtained for K_F values of 0.33, 0.51, and 0.57 at temperatures of 25°C, 40°C, and 50°C, respectively. The values of n, which are related to the distribution of ion $B(OH)^{4-}$ linked to the active sites on the adsorbent, were 1.392, 1.476, and 1.481, respectively, for 25°C, 40°C, and 50°C (Table 2).

The value of n is a constant that indicates the strength of adsorption and is also known as a measure of linearity since n is equal to one. In this case, the adsorption process is linear; therefore, the adsorption sites are homogeneous concerning energy, and there would not be any interactions between the adsorbate and the adsorbent. For values of n smaller than the unit, the connection between the adsorbate and the adsorbent is very weak, and consequently, the process is not favorable for the adsorption and its adsorptive capacity decreases.

However, for values of n greater than the unit, the adsorption process is favorable; therefore, the adsorption capacity increases, indicating that the adsorption of ions is favorable under experimental conditions studied [41–43]. As seen in Table 3, all values of n are greater than the unit for the Freundlich isotherm, and the temperature increases from 25°C to 50°C, indicating that the adsorption of boron MgO-500 is favored by the temperature.

Table 3: Isotherm constants of the Freundlich isotherm (K_F, n) for the adsorption of boron in different adsorbents.

Adsorbent	K_F	n	Reference
Mining tailing (Woolley Edge)	0.004	1.4	[42]
Pural (76% Al_2O_3)	0.031	0.6	[41]
Siral (28% SiO_2, 72% Al_2O_3)	0.057	1.3	[41]
Activated alumina	0.440	1.4	[42]
MgO	0.570	1.5	Present work
Al_2O_3 (72%) and SiO_2 (28%)	0.057	1.3	[41]
N-methyl-D-glucamine onto SPC	0.282	2.3	[23]
Tannin gel	0.113	1.4	[44]

It can also be noticed from Table 3 that the adsorption constants (K_F) for boron removal process at different temperatures are higher than those obtained for boron removal processes with activated charcoal, activated alumina, Pural (76% Al_2O_3), Siral (28% SiO_2, 72% Al_2O_3), tannin gel, and mineral wastes. It is clear that the capacity of boron adsorption by MgO is higher than other adsorbents with exception to N-methyl-D-glucamine onto SPC and neutralized red mud.

3.3. Kinetic Analysis. The kinetics of boron removal by adsorption onto MgO was studied in the present work. The rate in which boron is removed by adsorption is the most important parameter for the design of a continuous or batch system in an effluent treatment plant. Therefore, it is essential to establish the dependency of time in the adsorption process for different operational conditions.

The kinetics of adsorption depends on the adsorbate-adsorbent interaction. The rate of adsorbate removal determines the residency time required for complete adsorption and could be calculated by kinetic analysis.

3.3.1. Equilibrium Kinetics. During an adsorption process, the sorbed solute tends to desorb and return to the solution, and vice versa. The process occurs continuously until, at a given time, the adsorption and desorption rates reach an equilibrium state. Hence, in this stage, there will not be any additional adsorption of the pollutant in the solution [45–47].

Tests were conducted to determine the equilibrium of the reaction under the following conditions: 500 mL solution with a concentration of 350 mg·L^{-1} of boron was prepared; then, MgO was added to obtain a concentration of 40 g·L^{-1}, maintaining the pH at 10 and stirring speed of 150 rpm. Samples were collected at different time periods (5, 10, 15, 20, 25, 30, 40, 50, 60, 90, 140, 190, and 240 min).

Figure 5 shows the effect of temperature on boron removal.

The maximum adsorption capacities were 7.2, 7.7, and 8.0 mg·g^{-1} at temperatures of 25°C, 40°C, and 50°C, respectively.

It can also be observed, according to Figure 5, that the rate of the process is greatly affected by an increase in temperature, and at 25°C, 40°C, and 50°C, the equilibrium of reaction was reached around 40 min, 30 min, and 15 min,

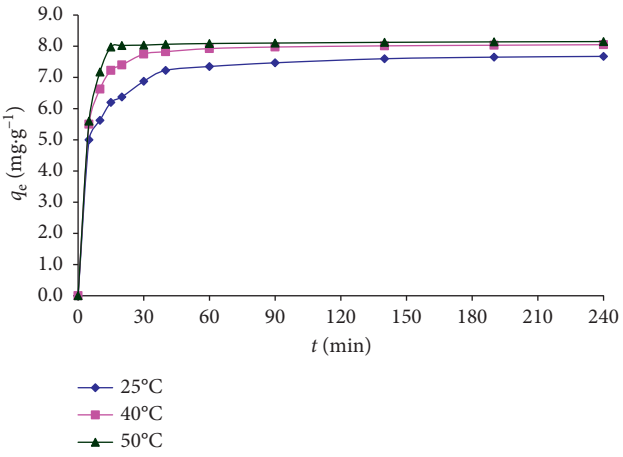

Figure 5: Profile of boron adsorption time as a function of temperature. Boron concentration = 350 mg·L^{-1}, pH = 10, MgO concentration = 40 g·L^{-1}, and stirring speed = 150 rpm.

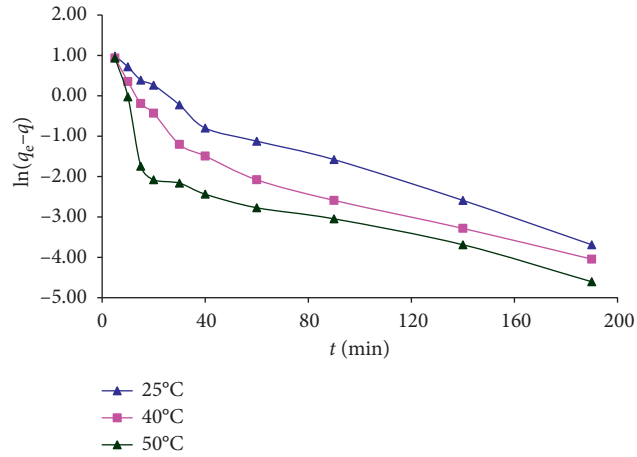

Figure 6: Application of the kinetic results to the pseudo-first-order model at temperatures of 25°C, 40°C, and 50°C. Concentration of boron = 350 mg·L^{-1}, pH = 10, concentration of MgO = 40 g·L^{-1}, and stirring speed = 150 rpm.

respectively. From this stage, the variations in adsorption capacities were insignificant. Figure 5 also shows that the period of time for reaching equilibrium at temperatures of 40°C and 50°C is relatively short, which could be an advantage for future industrial applications.

3.3.2. Kinetic Models. In 1898, Lagergren presented the kinetic model known as "pseudo-first-order equation" for a liquid-solid system based on the adsorption capacity of the solid.

Later, Ho and Mckay [46] presented a modification of the Lagergren model based on the concentration of the pollutant in the solution, known as "pseudo-second-order equation."

Next, a kinetic analysis based on those models will be presented, which are the most usual and well-established ones for this type of adsorption process.

(1) Pseudo-First-Order Kinetic Model. The Lagergren model was developed for solid-liquid adsorption systems and is based on the adsorption capacity of the adsorbent. Equation (7) shows how this model is usually expressed, being one of the most used models to study the kinetics of adsorption processes:

$$\log(q_m - q_t) = \log(q_m) - \frac{k}{2.303}t. \quad (7)$$

Figures 6 and 7 present the application of the experimental data to the pseudo-first-order model at 25°C, 40°C, and 50°C, respectively.

It is observed in Figure 6 that there is an apparent multilinearity of the kinetic curves, which may lead us to think that the process happens in two stages. Figure 7 shows the good fit of the experimental kinetic data at 25°C in the pseudo-first-order model with $R^2 = 0.96$.

(2) Pseudo-Second-Order Kinetic Model. The pseudo-second-order model is based on the concentration of the

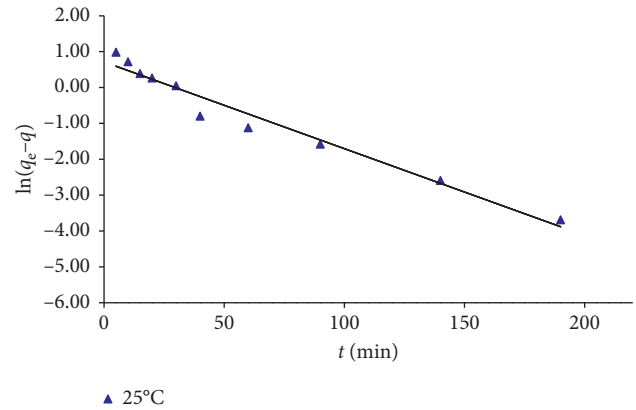

Figure 7: Adjustment of the adsorption data to the pseudo-first-order model at 25°C. Concentration of boron = 350 mg·L^{-1}, pH = 10, concentration of MgO = 40 g·L^{-1}, and stirring speed = 150 rpm.

pollutant in the solution. The adsorption rate equation can be written as follows:

$$\frac{t}{q_t} = \frac{1}{kq_e^2} + \frac{1}{q_e}t, \quad (8)$$

where k is the adsorption rate constant (g·mg^{-1}·min^{-1}), q_e is the concentration of boron adsorbed at equilibrium (mg·g^{-1}), and q_t is the concentration of boron on the surface of the adsorbent at time t (mg·g^{-1}). The constants can be determined experimentally by plotting t/q_t versus t.

Figure 8 illustrates the adjustment of the experimental data to the pseudo-second-order kinetic model. Table 4 presents the values of the kinetic parameters obtained from this setting.

It can be observed from the values presented in Table 4 that the pseudo-second-order model is the one with the best fit of the experimental data of the adsorption process, since R^2 values of 0.99 were obtained for this model at the three temperatures studied (25°C, 40°C, and 50°C) compared to

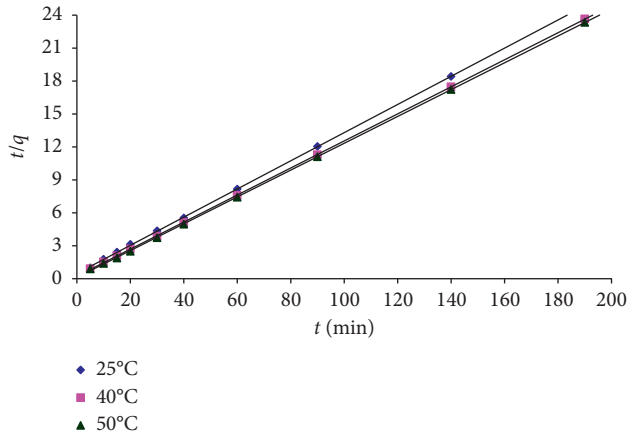

FIGURE 8: Adjustment of the adsorption data to the pseudo-second-order model at 25°C, 40°C, and 50°C. Boron concentration = 350 mg·L^{-1}, pH = 10, concentration of MgO = 40 g·L^{-1}, and stirring speed = 150 rpm.

the R^2 values obtained for the pseudo-first-order model of 0.96, 0.83, and 0.43 at the same temperatures, respectively.

The values of q_e obtained at 25°C, 40°C, and 50°C by the pseudo-second-order model were 7.81 mg·g^{-1}, 8.12 mg·g^{-1}, and 8.17 mg·g^{-1}, respectively, while the experimental values obtained at the same temperatures were 7.23 mg·g^{-1}, 7.75 mg·g^{-1}, and 7.98 mg·g^{-1}, respectively. It can be observed from the comparison of the values of q_e obtained experimentally and by the pseudo-second-order model that the values of q_e are very similar, which confirms that the process of removal of boron by adsorption with MgO follows a pseudo-second-order kinetics.

Studies available in the literature show that many models provide a clarification for the overall adsorption process. However, in many cases, that is not possible when graphs present multilinear feature [48].

In order to understand these cases, it is usual to divide the graph into two or more straight lines and to suggest that the adsorption mechanism is controlled by each straight line. This practice may help to understand the adsorption mechanism to some extent [48].

From Figure 6, which represents the application of the experimental data to a pseudo-first-order kinetic model, it is observed that the adsorption process at the three temperatures seems to occur in two stages due to the two straight slopes obtained from the application of the model, which is confirmed by the adjustment of the results to the pseudo-second-order model that describes a two-step reaction occurring consecutively.

3.3.3. Apparent Activation Energy. The apparent activation energy of the adsorption process was calculated. The variation in the rate constant according to an increase in temperature can be described by the Arrhenius equation (9):

$$k = k_o \exp^{(-E_A/RT)}, \tag{9}$$

where k is the sorption rate constant (g·mg^{-1}·min^{-1}), k_o is the independent factor of temperature (g·mg^{-1}·min^{-1}), E_A is the adsorption activation energy (kJ·mol^{-1}), R is the gas constant (8.314 J·mol^{-1}·K^{-1}), and T is the temperature of the solution (K).

Equation (10) can be expressed in linear form as follows:

$$\ln k = \ln A - \left(\frac{E_A}{R}\right) \cdot \left(\frac{1}{T}\right). \tag{10}$$

As shown in Figure 8, there is a linear correlation between the rate constant of the pseudo-second-order model and its corresponding absolute temperature, with a correlation coefficient of 0.98. Figure 9 shows the correlated experimental data in the linearized Arrhenius equation. From Figure 9, the relation between k and T can be represented as follows:

$$k = 3.02 \times 10^6 \exp^{(-45.54/8.314T).} \tag{11}$$

From (11), we can observe that the frequency factor A is 3.02×10^6 g·mg^{-1}·min^{-1}, and the activation energy is 45.54 kJ·mol^{-1}, which is very slightly outside of the suggested normal range (8–40 kJ·mol^{-1}) for a typical physical adsorption processes [49–52].

3.4. Thermodynamics of the Process. In order to understand the thermodynamics of the process of boron removal by adsorption with MgO, some thermodynamic parameters were determined. Adsorption tests at different temperatures were performed using a thermostatic bath, under the following conditions: initial boron concentration = 350 mg·L^{-1}, pH = 10, MgO concentration = 40 g·L^{-1}, and stirring speed = 150 rpm.

The temperatures studied were 25°C, 40°C, and 50°C, and the parameters calculated were standard Gibbs free energy variation (ΔG°), standard enthalpy variation (ΔH°), and standard entropy variation (ΔS°).

The standard free energy variation in the adsorption process is related to the equilibrium constant (K_c) and can be calculated according to the following equation:

$$\Delta G^\circ = RT \ln K_c, \tag{12}$$

where R is the gas constant (8.314 J·mol^{-1}·K^{-1}), T is the absolute temperature, and K_c is the equilibrium constant, which can be estimated from the following equation:

$$K_c = \frac{C_s}{C_e}, \tag{13}$$

where C_e is the concentration of boron at equilibrium in the solution (mg·L^{-1}) and C_s is the concentration of boron at equilibrium in the adsorbent (mg·L^{-1}).

The variations in standard enthalpy (ΔH°) and standard entropy (ΔS°) can be calculated according to the following Van't Hoff equation:

$$\ln K_c = \frac{\Delta S^\circ}{R} - \frac{\Delta H^\circ}{RT}. \tag{14}$$

Figure 9 represents the plot of $\ln K_c$ versus $1/T$ from the Van't Hoff equation, where the slope of the line is $-\Delta H^\circ/R$ and the intercept with y-axis is $\Delta S^\circ/R$, from which the

Table 4: Kinetic parameters for the adsorption of boron with MgO at 25°C, 40°C, and 50°C.

Temperature	Pseudo-first-order model			Pseudo-second-order model			
	q_e (mg·g^{-1})	k (min^{-1})	R^2	q_e (mg·g^{-1})	k (g·mg min^{-1})	V_o (g·mg min^{-1})	R^2
25°C	5.158	0.056	0.96	7.81	0.033	2.012	0.99
40°C	—	—	0.83	8.12	0.067	4.409	0.99
50°C	—	—	0.46	8.17	0.141	9.381	0.99

Concentration of boron = 350 mg·L^{-1}, pH = 10, concentration of MgO = 40 g·L^{-1}, and stirring speed = 150 rpm.

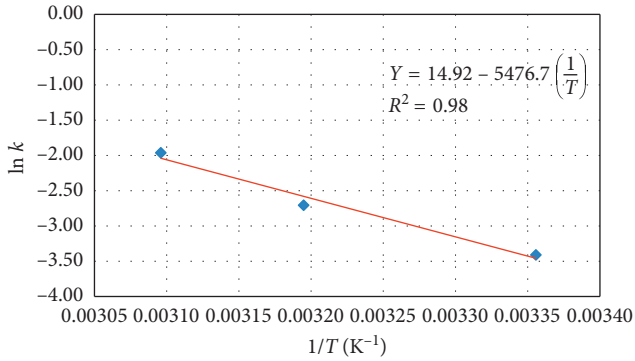

Figure 9: Variation of ln (k) versus 1/T.

corresponding thermodynamic parameters were obtained and are presented in Table 5.

From Table 5, it can be observed that when the temperature of the adsorption process increases from 25°C to 40°C and from 40°C to 50°C, the ΔG° values become increasingly negative varying from −4.16 kJ·mol^{-1} to −5.88 kJ·mol^{-1} and from −5.88 kJ·mol^{-1} to −6.26 kJ·mol^{-1}, respectively. That means the process is spontaneous at all temperatures due to the negative value of ΔG°. Likewise, as the temperature increases, the $B(OH)_4^-$ ion has higher affinity to be adsorbed by MgO.

The ΔG° for physical sorption is between −20 and 0 kJ·mol^{-1} and is ranged from −80 to −400 kJ·mol^{-1} for chemical sorption [52, 53]. The values of ΔG° presented in Table 5 indicate that the sorption process is controlled by physical adsorption.

The adsorption enthalpy is also a parameter used to indicate the intensity of the interaction between the adsorbate and the adsorbent. In the phenomenon of physisorption, this parameter has low values (up to about 40 kJ·mol^{-1}) since it is characterized by a low degree of interaction, being the forces involved of the order of magnitude of van der Waals forces. The chemisorption phenomenon is characterized by a high degree of interaction between the adsorbate and the surface of the adsorbent; the enthalpy values, in this case, are around 800 kJ·mol^{-1} [51]. The ΔH° calculated in this work was 21.75 kJ mol^{-1}·K^{-1}, indicating that the sorption process is controlled by physical adsorption.

Positive value of ΔS° (87.33 kJ·mol^{-1}) indicates that the degrees of freedom increase at the solid-liquid interface during the adsorption of boron onto magnesium oxide particles.

Table 5: Thermodynamic parameters for the adsorption of boron with MgO at 25°C, 40°C, and 50°C.

Temperature	K_c	ΔG° (kJ·mol-1)	H° (kJ·mol^{-1}·K^{-1})	ΔS° (kJ·mol^{-1})
25°C	5.36	−4.16	21.75	87.33
40°C	9.61	−5.88	–	–
50°C	10.29	−6.26	–	–

Concentration of boron = 350 mg·L−1, pH = 10, concentration of MgO = 40 g·L−1, stirring speed = 150 rpm, and time = 240 min. The positive value of the standard enthalpy ΔH° = 21.75 kJ·mol^{-1}·K^{-1} for boron adsorption onto MgO shows the endothermic feature.

4. Conclusions

Equilibrium, kinetics, and thermodynamic studies for the adsorption of boron onto magnesium oxide powder were carried out.

The experimental data of adsorption were conducted by the Langmuir, Freundlich, and DR models, wherein the Freundlich isotherm was found to have a better fit for the equilibrium data for adsorption of boron under ambient temperature (25°C) and at higher temperatures (40°C and 50°C), respectively.

Additionally, the investigation of the kinetics of the overall adsorption process was conducted for the pseudo-first-order kinetic and pseudo-second-order kinetic models. Results show that the pseudo-second-order kinetic model generates the best fit to all experimental data. Such result suggests that the adsorption process at these temperatures seems to occur in two stages due to the two straight slopes obtained through the application of the pseudo-first-order kinetic model, which is confirmed by the adjustment of the results to the pseudo-second-order model.

The calculated activation energy (E_a) was 45.54 kJ·mol^{-1}, which is very slightly outside the normal range (8–40 kJ·mol^{-1}) for a typical physical adsorption process.

The values calculated for ΔG° and ΔH° were −4161.43 kJ·mol^{-1} and 21.75 kJ·mol^{-1}, respectively. These values confirm the spontaneous and endothermic nature of the process and also suggest a physical adsorption process.

Data Availability

The boron analysis data used to support the findings of this study are available from the corresponding author upon request.

Conflicts of Interest

The authors declare that there are no conflicts of interest regarding the publication of this paper.

Acknowledgments

The funding for this research was provided by the Research and Development Center of Petrobras and the National Council for Scientific and Technological Research of Brazil (CNPq). The authors thank Mariana Lima for assistance during the experimental work.

References

[1] G. Kelvin and M. M. Arvind, "Current perspective on produced water management challenges during hydraulic fracturing for oil and gas recovery," *Environmental Chemistry*, vol. 12, no. 3, pp. 261–266, 2015.

[2] H. E. Ezerie, H. I. Mohamed, and R. B. M. K. Shamsul, "Boron in produced water: challenges and improvements: a comprehensive review," *Journal of Applied Sciences*, vol. 12, no. 5, pp. 402–415, 2012.

[3] F. A. F. Cedric, J. S. Vincent, A. M. Bruce, and M. Farshid, "Determination of boron in produced water using the carminic acid assay," *Talanta*, vol. 150, pp. 240–252, 2016.

[4] H. E. Ezerie, H. I. Mohamed, R. M. K. Shamsul, and Y. Asim, "Boron removal from produced water using electrocoagulation," *Process Safety and Environmental Protection*, vol. 92, no. 6, pp. 509–514, 2014.

[5] P. Howe, "A review of boron effects in the environment," *Biological Trace Element Research*, vol. 66, no. 1–3, pp. 153–165, 1998.

[6] J. Parks and M. Edwards, "Boron in the environment," *Critical Reviews in Environmental Science and Technology*, vol. 35, no. 2, pp. 81–114, 2005.

[7] Brazilian NR, *Conama 357 Resolution*, National Environment Council of Brazil, São Paulo, SP, Brazil, 2017, http://www.mma.gov.br/port/conama/.

[8] MINAM, *Ministry of Environment of Peru*, November 2017, http://sinia.minam.gob.pe/normas.

[9] W. Boyang, G. Xianghai, and B. Peng, "Removal technology of boron dissolved in aqueous solutions–A review," *Colloids and Surfaces A*, vol. 444, p. 338, 2014.

[10] C. T. Onur, V. Jan, and T. Cengiz, "Constructed wetlands for boron removal: a review," *Ecological Engineering*, vol. 64, pp. 350–359, 2014.

[11] WHO, *Guidelines for Drinking-Water Quality*, World Health Organization, Geneva, Switzerland, 4th edition, 2011.

[12] H. E. Ezerie, H. I. Mohamed, R. M. K. Shamsul, and A. Zubair, "Electrochemical removal of boron from produced water and recovery," *Journal of Environmental Chemical Engineering*, vol. 3, no. 3, pp. 1962–1973, 2015.

[13] G. Zhimin, L. Jiafei, B. Peng, and G. Xianghai, "Boron removal from aqueous solution by adsorption–A review," *Desalination*, vol. 383, pp. 29–37, 2016.

[14] K. Tomohito, O. Jumpei, and Y. Toshiaki, "Use of Mg-Al oxide for boron removal from an aqueous solution in rotation: kinetics and equilibrium studies," *Journal of Environmental Management*, vol. 165, pp. 280–285, 2016.

[15] J. Kluczka, T. Korolewicz, M. Zołotajkin, W. Simka, and M. Raczek, "A new adsorbent for boron removal from aqueous solutions," *Environmental Technology*, vol. 34, no. 11, pp. 1369–1376, 2013.

[16] K. Maciej, B. Z. Barbara, D. Piotr, and T. Marian, "The concept of a system for electrodialytic boron removal into alkaline concentrate," *Desalination*, vol. 310, pp. 75–80, 2013.

[17] C. Zhifan, A. T. Alicia, R. A. Savina, X. Junliang, and T. Y. Norman, "Removal of boron from wastewater: evaluation of seven poplar clones for B accumulation and tolerance," *Chemosphere*, vol. 167, pp. 146–154, 2017.

[18] C. T. Onur, T. Cengiz, B. Harun, C. Arzu, and Y. Anıl, "Role of plants and vegetation structure on boron (B) removal process in constructed wetlands," *Ecological Engineering*, vol. 88, pp. 143–152, 2016.

[19] P. Qingyun, M. A. Ibrahim, and H. Zhen, "Enhanced boron removal by electricity generation in a microbial fuel cell," *Desalination*, vol. 398, pp. 165–170, 2016.

[20] P. Qingyun, M. A. Ibrahim, and H. Zhen, "Mathematical modeling based evaluation and simulation of boron removal in bioelectrochemical systems," *Science of the Total Environment*, vol. 570, pp. 1380–1389, 2016.

[21] K. Nalan, K. Pelin, Y. Duygu, Y. Ümran, and Y. Mithat, "Coupling ion exchange with ultrafiltration for boron removal from geothermal water-investigation of process parameters and recycle tests," *Desalination*, vol. 316, pp. 17–22, 2013.

[22] N. Hilal, G. J. Kim, and C. Somerfield, "Boron removal from saline water: a comprehensive review," *Desalination*, vol. 273, no. 1, pp. 23–35, 2011.

[23] X. Li, R. Liu, S. Wua, J. Liu, S. Cai, and D. Chen, "Efficient removal of boron acid by N-methyl-D-glucamine functionalized silica–polyallylamine composites and its adsorption mechanism," *Journal of Colloid and Interface Science*, vol. 361, no. 1, pp. 232–237, 2011.

[24] J. Wolska and M. Bryjak, "Methods for boron removal from aqueous solutions—A review," *Desalination*, vol. 310, pp. 18–24, 2013.

[25] E. Güler, C. Kaya, N. Kabay, and M. Arda, "Boron removal from seawater: State-of-the-art review," *Desalination*, vol. 356, pp. 85–93, 2015.

[26] E. Güler, N. Kabay, M. Yüksel, E. Yavuz, and U. Yüksel, "A comparative study for boron removal from seawater by two types of polyamide thin film composite SWRO membranes," *Desalination*, vol. 273, no. 1, pp. 81–84, 2011.

[27] N. Nadav, "Boron removal from seawater reverse osmosis permeate utilizing selective ion exchange resin," *Desalination*, vol. 124, no. 1–3, pp. 131–135, 1999.

[28] M. Simonnot, C. Castel, M. Nicolai, C. Rosin, M. Sardin, and H. Jauffret, "Boron removal from drinking water with a boron selective resin: is the treatment really selective?," *Water Research*, vol. 34, no. 1, pp. 109–116, 2000.

[29] N. Kabay, M. Bryjak, S. Scholosser, and M. Kitisa, "Adsorption-membrane filtration (AMF) hybrid process for boron removal from seawater: an overview," *Desalination*, vol. 223, no. 1–3, pp. 38–48, 2008.

[30] M. Tagliabue, A. Reverberi, and R. Bagatin, "Boron removal from water: needs, challenges and perspectives," *Journal of Cleaner Production*, vol. 77, pp. 56–64, 2014.

[31] J. Cao, S. Monroe, and D. Hendry, "Environmentally preferred process for efficient boron and hardness removal for produced water reuse," in *Proceedings of SPE Annual Technical Conference and Exhibition*, Houston, TX, USA, 2015.

[32] Petrobras Transporte SA, July 2017, http://www.transpetro.com.br/pt_br/areas-de-negocios/terminais-e-oleodutos/terminais-aquaviarios.html.

[33] Z. Jin, Y. Jia, K. Zhang et al., "Effective removal of fluoride by porous MgO nanoplates and its adsorption mechanism," *Journal of Alloys and Compounds*, vol. 675, pp. 292–300, 2016.

[34] Z. Bai, Y. Zheng, and Z. Zhang, "One-pot synthesis of highly efficient MgO for the removal of Congo red in aqueous solution," *J. Mater. Chem. A*, vol. 5, pp. 6630–6637, 2017.
[35] M. Dubinin and L. Radushkevich, "Equation of the characteristic curve of activated charcoal," *Proceedings of the USSR Academy of Sciences*, vol. 55, pp. 331–333, 1947.
[36] I. Langmuir, "The constitutional and fundamental properties of solids and liquids,," *Journal of the American Chemical Society*, vol. 38, no. 11, pp. 2221–2295, 1916.
[37] H. Freundlich, "Over the adsorption in solution," *Zeitschrift für Physikalische Chemie*, vol. 57, pp. 385–470, 1906.
[38] C. H. Giles, A. P. D´Silva, and A. S. Trivedi, *Surface Area Determination*, Butterworth, London, UK, 1970.
[39] R. Masel, *Principles of Adsorption and Reaction on Solid Surfaces*, Wiley, New York, NY, USA, 2nd edition, 1951.
[40] S. Goldberg, "Reactions of boron with soils," *Plant and Soil*, vol. 193, no. 2, pp. 35–48, 1997.
[41] Y. Seki, S. Seyhan, and M. Yurdakoc, "Removal of boron from aqueous solution by adsorption on Al_2O_3 based materials using full factorial design," *Journal of Hazardous Materials*, vol. 38, pp. 60–66, 2006.
[42] Y. Cengeloglu, "Removal of boron from aqueous solution by using neutralized red mud," *Journal of Hazardous Materials*, vol. 142, pp. 412–417, 2007.
[43] R. Sivaraj and C. Namasivayam, "Orange peel as an adsorbent in the removal of acid violet 17 (acid dye) from aqueous solutions," *Waste Management*, vol. 21, no. 1, pp. 105–110, 2001.
[44] S. Morisada, T. Rin, T. Ogata, KY. Ho, and Y. Nakano, "Adsorption removal of boron in aqueous solutions by amine-modified tannin gel," *Water Research*, vol. 45, no. 13, pp. 4028–4034, 2011.
[45] P. Cheremisinoff, *Water and Water Pollution Handbook*, Wiley, New York, NY, USA, 2nd edition, 2002.
[46] Y. S. Ho and G. McKay, "A comparison of chemisorption kinetic models applied to pollutant removal on various sorbents," *Process Safety and Environmental Protection*, vol. 76, no. 4, pp. 332–340, 1998.
[47] Metcalf and Eddie, *Wastewater Engineering: Treatment, Disposal, and Reuse*, McGraw-Hill, Inc., Boston, MA, USA, 4th edition, 2003.
[48] X. Yang and B. Al-Duri, "Kinetic modeling of liquid-phase adsorption of reactive dyes on activated carbon," *Journal of Colloid and Interface Science*, vol. 287, no. 1, pp. 25–34, 2005.
[49] U. Isah, G. Abdulraheem, S. Bala, S. Muhammad, and M. Abdullahi, "Kinetics, equilibrium and thermodynamics studies of C.I. Reactive Blue 19 dye adsorption on coconut shell based activated carbon," *International Biodeterioration and Biodegradation*, vol. 102, pp. 265–273, 2015.
[50] A. Elekli, G. lgüna, and H. Bozkurtb, "Sorption equilibrium, kinetic, thermodynamic, and desorption studies of Reactive Red 120 on Chara contraria," *Chemical Engineering Journal*, vol. 191, pp. 228–235, 2012.
[51] S. P. D. Monte Blanco, F. B. Scheufele, A. N. Módenes et al., "Kinetic, equilibrium and thermodynamic phenomenological modeling of reactive dye adsorption onto polymeric adsorbent," *Chemical Engineering Journal*, vol. 307, pp. 466–475, 2017.
[52] H. Nollet, M. Roels, P. Lutgen, P. Van der Meeren, and W. Verstraete, "Removal of PCBs from wastewater using fly ash," *Chemosphere*, vol. 53, no. 6, pp. 655–665, 2003.
[53] C. H. Wu, "Adsorption of reactive dye onto carbon nanotubes: Equilibrium, kinetics and thermodynamics," *Journal of Hazardous Materials*, vol. 144, no. 1-2, pp. 93–100, 2007.